

1 **Northern Hemisphere stratospheric winds in higher midlatitudes:**
2 **longitudinal distribution and long-term trends**

3

4 **Michal Kozubek, Peter Krizan, Jan Lastovicka**

5

6 Institute of Atmospheric Physics ASCR, Bocni II, 14131 Prague, Czech Republic

7 Correspondence to: M. Kozubek (kom@ufa.cas.cz)

8

9

10

11

12

13

14

15

16

17

18

19

20

21

22

23

24

25

26

27

28

29

30

31

32

33

34 **Abstract**

35 The Brewer-Dobson circulation (BDC, mainly meridional circulation) is very
36 important for stratospheric ozone dynamics and, thus, for the overall state of the stratosphere.
37 There are some indications that the meridional circulation in the stratosphere could be
38 longitudinally dependent, which would have an impact on the ozone distribution. Therefore,
39 we analyse here the meridional component of the stratospheric wind at northern middle
40 latitudes to study its longitudinal dependence. The analysis is based on the NCEP/NCAR-1
41 (National Centres for Environmental Prediction and the National Centre for Atmospheric
42 Research), MERRA (Modern Era-Retrospective Re-Analysis) and ERA-Interim (European
43 Centre for Medium-Range Weather Forecasts (ECMWF) Re-Analysis Interim) reanalysis
44 data. The well-developed, two-core structure of strong but opposite meridional winds, one at
45 each hemisphere at 10 hPa at higher northern middle latitudes, and a less-pronounced five-
46 core structure at 100 hPa, are identified. In the central areas of the two-core structure the
47 meridional and zonal wind magnitudes are comparable. The two-core structure at 10 hPa is
48 almost identical for all three different reanalysis data sets in spite of the different time periods
49 covered. The two-core structure is not associated with tides. However, the two-core structure
50 at the 10 hPa level is related to the Aleutian pressure high at 10 hPa. Zonal wind, temperature
51 and the ozone mixing ratio at 10 hPa also exhibit the effect of the Aleutian high, which thus
52 affects all parameters of the northern hemisphere middle stratosphere. Long-term trends in the
53 meridional wind in the “core” areas are significant at the 99% level. Trends of meridional
54 winds are negative during the period of ozone depletion development (1970-1995), while they
55 are positive after the ozone trend turnaround (1996-2012). Meridional winds trends are
56 independent of the Sudden Stratospheric Warming (SSW) occurrence and the quasi-biennial
57 oscillation (QBO) phase. The influence of the 11-year solar cycle on stratospheric winds has
58 been identified only during the west phase of QBO. The well-developed two-core structure in

59 the meridional wind illustrates the limitations of application of the zonal mean concept in
60 studying stratospheric circulation.

61

62

63 **1. Introduction**

64

65 Stratospheric winds play an important role in stratospheric chemistry through the transport of
66 long-lived species, but they could also create transport barriers, which could isolate the polar
67 vortex in winter (Shepherd, 2007, 2008). Simultaneously with the chemical processes, the
68 trace gas distribution modulates the radiative forcing in the stratosphere. The changes of
69 stratospheric wind, namely the strengthening of the westerly polar vortex and its poleward
70 shift, are coupled with ozone depletion and temperature changes (Scaife et al., 2012). For
71 example, the unprecedented ozone loss in the Arctic in 2011 was caused by extreme
72 meteorological conditions (e.g., Pommereau et al., 2013, Manney et al., 2011). The Antarctic
73 ozone hole intensification over the 1980–2001 period is not solely related to the trend in
74 chemical losses, but more specifically to the balance between the trends in chemical losses
75 and ozone transport (Monier and Weare, 2011a). One of the most studied circulation
76 structures in the stratosphere is the Brewer-Dobson circulation (BDC). A detailed description
77 of this circulation can be found in Butchart (2014). Many model studies reveal an acceleration
78 of the residual mean circulation and the Brewer-Dobson circulation due to the increasing
79 greenhouse gas (GHG) concentration (Oberlander et al., 2013; Lin and Fu, 2013; Oman et al.,
80 2009). However, the age of air data does not confirm a simple pattern of reduction of the age
81 of air as a consequence of the Brewer-Dobson circulation intensification (Engel et al., 2009;
82 Stiller et al., 2012, Waugh and Hall, 2002). The most recent complex analysis of
83 observational information reveals a reduction of the age of air in the lower stratosphere but an
84 opposite effect in the middle and upper stratosphere (Ray et al., 2014). Monier and Weare

85 (2011b) found some weakening of the northern winter Brewer-Dobson circulation in the polar
86 region in reanalyses ERA-40 (ECMWF Re-analysis for 40 years) and R-2 (NCEP-
87 DOE Reanalysis 2). Some changes of stratospheric wind (strengthening of the westerly polar
88 vortex and its poleward shift, changes in the Brewer-Dobson circulation) are coupled with
89 ozone depletion and also temperature changes. Possible interactions between changes in the
90 stratospheric dynamics and climate changes in the troposphere have been described by
91 Hartmann et al. (2000), Scaife et al. (2012) and Deckert and Dameris (2008). The
92 stratospheric QBO and downward feedback from the stratospheric vortex to tropospheric
93 weather systems have been reported to be relevant both in the context of weather prediction
94 and climate (Baldwin and Dunkerton, 1999; Baldwin et al., 2003; Sigmond et al., 2008;
95 Marshall and Scaife, 2009; Wang and Chen, 2010). Moreover, stratospheric wind (zonal and
96 meridional) affects vertically propagating atmospheric waves, which control the transport
97 circulation in the stratosphere and mesosphere (Holton and Alexander, 2000).

98 It is generally accepted that the meridional wind component in the stratosphere is
99 much weaker than the zonal wind component. However, as we show later, it is not always the
100 case. Many studies use zonal mean winds for their analyses. The Northern Hemisphere has a
101 pronounced distribution of continents, mountain regions and oceans, which is reflected in the
102 troposphere and also in the stratosphere. Some phenomena introduce longitudinal differences
103 into wind pattern, for example the El-Nino Southern Oscillation - ENSO (e.g., Weare, 2010).
104 The total ozone in the winter higher middle latitudes has a strong longitudinal dependence, the
105 maximum-minimum difference being more than 100 Dobson Units (D.U.) (e.g., Mlch, 1994).
106 Bari et al. (2013) found longitudinal dependence of residual winds in the stratosphere and,
107 through impact on the Brewer-Dobson circulation, changes in global circulation, distributions
108 and concentration of stratospheric ozone and water vapour in the stratosphere and lower
109 mesosphere for 2001-2006. Therefore we study the longitudinal structure of meridional wind

110 (and other parameters) in the stratosphere as a phenomenon of non-zonality, and the long-
111 term evolution of this longitudinal structure, based on the long-term reanalyses data series.
112 This is the main aim of this paper.

113 Our study of longitudinal distribution of meridional and zonal wind should reveal if
114 and where the meridional wind is comparable to the zonal wind. The results could have an
115 impact on BDC circulation in terms of longitudinal distribution, which is very important for
116 ozone transport in the stratosphere. The distribution of meridional wind is among others very
117 important for wave propagation in the stratosphere (Matsuno, 1970, Kodera et al., 1990).

118 To test the temporal stability of longitudinal distribution, long-term trends at latitudes
119 of the most pronounced longitudinal structures are calculated. Ozone concentration in the
120 northern middle latitudes changed its trend (from negative to positive) in the mid-1990s (e.g.,
121 Harris et al., 2008). Since ozone is the main contributor to heating of the stratosphere via
122 absorption of solar radiation, this turnaround of ozone trend had also to affect the behaviour
123 of other stratospheric parameters (changes in temperature and wind trends), and it affects even
124 the mesosphere and lower thermosphere (e.g., Lastovicka et al., 2012). Since ozone trends in
125 the northern middle latitudes changed in the mid-1990s (e.g., Harris et al., 2008), trends in
126 stratospheric dynamics are expected to be altered by the ozone recovery and thus trends in the
127 periods before and after the mid-1990s are examined separately.

128 SSW and the QBO are known to have an important impact on the stratosphere,
129 including its circulation (Limpasuvan et al. 2004, Naito and Hirota, 1997, Labitzke and van
130 Loon, 1988). The stratosphere is also influenced by solar activity (e.g., Gray et al., 2010 and
131 references herein). Impact of these phenomena on stratospheric circulation, particularly on the
132 observed longitudinal structures in meridional wind, deserves attention and analysis.

133 This paper focuses on two topics:

134 (1) Longitudinal distribution of the meridional wind component at different pressure
135 levels and the possible reasons for its behaviour. Therefore the longitudinal distributions of
136 geopotential height and zonal wind component will also be calculated. This will be
137 accompanied by trend analysis of observed longitudinal structures. The results of the
138 meridional wind distribution analysis are described in Section 3.1. Long-term trends in the
139 longitudinal distribution of meridional wind are also examined and the results are presented in
140 Section 3.2.

141 (2) Trend analysis of stratospheric total horizontal wind and meridional component
142 with connection to QBO, SSW (mainly wave driven) and solar activity. The results are
143 described in Section 3.3.

144 The structure of the paper is as follows. In Section 2, the data and methods are
145 described. Then, in Section 3, the results of analysis are shown and, in Section 4, they are
146 briefly discussed. Section 5 summarizes conclusions.

147

148 **2. Data and methods**

149

150 Stratospheric winds have been measured from the ground using active and passive techniques
151 (Hildebrand et al., 2012; Rüfenacht et al., 2012). From space they were measured by the High
152 Resolution Doppler Imager (HRDI) on the Upper Atmospheric Research Satellite (UARS)
153 covering 10–35 km and 60°S–60°N, using the molecular oxygen A- and B-bands (Ortland et
154 al., 1996). Baron et al. (2013) derived winds from SMILES (Superconducting Submillimetre-
155 wave Limb-Emission Sounder). However, direct wind measurements from satellite do not
156 provide sufficiently long and homogeneous global data series.

157 Therefore when studying longitudinal distribution of meridional or zonal wind, we use
158 three independent reanalyses data, namely NCEP/NCAR-1 reanalysis (National Centers for

159 Environmental Prediction and the National Center for Atmospheric Research, further on
160 NCEP/NCAR), MERRA (Modern Era-Retrospective Re-Analysis) and ERA-Interim
161 (European Centre for Medium-Range Weather Forecasts (ECMWF) Re-Analysis Interim).
162 The NCEP/NCAR reanalysis was described in detail by Kistler et al. (2001). This reanalysis
163 provides data from 1948 onwards (but the data is more reliable from 1957 onwards, when the
164 first upper-air observations were established) and better global data from 1979 onwards, due
165 to the start of satellite data assimilation. Data is available on the 2.5° to 2.5° grid at 00, 06, 12
166 and 18 UTC. Vertical resolution is 28 levels from 1000 hPa to the top of the model at 2.7 hPa.
167 The NCEP/NCAR reanalysis system assimilates upper-air observations but it is only
168 marginally influenced by surface observations because model orography differs from reality
169 (Kistler et al., 2001). The ERA-Interim is described by Dee et al. (2011). Data is available
170 from 1979 on the 0.75° to 0.75° grid at 00, 06, 12 and 18 UTC. Vertical resolution is 60 levels
171 from 1000 hPa to the top of the model at 1 hPa. The MERRA reanalysis is described in and
172 downloaded from <http://disc.sci.gsfc.nasa.gov>. Data is available from 1979 on the 1.25° to
173 1.25° grid at 00, 06, 12 and 18 UTC. Vertical resolution is 42 levels from 1000 hPa to the top
174 of the model at 0.1 hPa.

175 According to Kozubek et al. (2014), stratospheric winds from the NCEP/NCAR
176 reanalysis are better for long-term trend analysis than those from ERA-40 and ERA-Interim
177 reanalyses - if we take into account the length of available period. Neither ERA-40, nor ERA-
178 Interim, nor MERRA separately cover the whole period 1958-2012. On the other hand,
179 general pattern and long-term changes of stratospheric winds in NCEP/NCAR, ERA-40 and
180 ERA-Interim reanalyses (except for the last four years of ERA-40) do not differ in main
181 features from each other since about 1970 (Kozubek et al., 2014), therefore it is possible to
182 use only one of these three reanalyses for trend analysis. The 10.7cm solar radio flux (from
183 <http://www.esrl.noaa.gov/psd/data/correlation/solar.data>) is used for the solar cycle influence

184 analysis (solar max and solar min). The QBO data at 50 hPa is taken from [http://www.geo.fu-](http://www.geo.fu-berlin.de/en/met/ag/strat/produkte/qbo/)
185 [berlin.de/en/met/ag/strat/produkte/qbo/](http://www.geo.fu-berlin.de/en/met/ag/strat/produkte/qbo/) and SSW data is taken from [http://www.geo.fu-](http://www.geo.fu-berlin.de/en/met/ag/strat/produkte/northpole/index.html)
186 [berlin.de/en/met/ag/strat/produkte/northpole/index.html](http://www.geo.fu-berlin.de/en/met/ag/strat/produkte/northpole/index.html)

187 For the investigation of longitudinal distribution of meridional wind (two-core
188 structure – section 3.1), zonal wind or geopotential height we have computed averages
189 throughout the period 1970-2012 for every grid point from 20°N to 60°N and for every
190 month. Analysis of the wind speed distribution at 100 hPa (where we can identify influence of
191 the troposphere and study dynamics near the tropopause) and 10 hPa (which is a
192 representative level for the middle stratosphere and major stratospheric warming
193 determination) at 00 UTC or the meridional wind speed distribution at 00, 06 and 12 UTC (for
194 examining possible influence of diurnal and semidiurnal tides) has been done for all three
195 reanalyses.

196 The trend analysis is focused on middle latitudes (50°- 60°N), at the pressure level of
197 10 hPa, in order to investigate the behaviour of wind in the two-core structure area. We also
198 analyse the connection between QBO, SSW and solar activity versus dynamics (stratospheric
199 wind) at 10 hPa. In trend analyses we have used either total horizontal wind or v (meridional)
200 components separately. The total horizontal wind speed is calculated from gridded u (zonal)
201 and v (meridional) components.

202 The selected latitudes are separated for trend analysis into four sectors (100°E-160°E –
203 poleward wind core, 160°E-140°W- the sector of the Aleutian height, 140°W-80°W –
204 equatorward wind core and 80°W-100°E – the sector not affected by the two-core structure,
205 see Fig. 1 and section 3.1).

206 We look for trends or differences between different groups in each sector at 10 hPa.
207 The statistical significance threshold of trends has been set at the 95% level, which is the
208 standard significance level for analyses in meteorology (wind, temperature, etc.), and in some

209 trend analysis it is set also at the 99% level. We divide data of the whole period into several
210 groups according to QBO (east or west QBO phase) or solar cycle influence (solar maximum
211 years and solar minimum years) and for the trend analysis we divided data into two periods
212 (1970-1995, with decreasing ozone, and 1995-2012, with increasing ozone). We compute
213 trends separately for all these groups with a significance threshold of 95% or 99%.

214

215 **3. Results**

216 *3.1 Longitudinal distribution of stratospheric meridional winds*

217 The whole period averages of meridional wind component for each grid point from
218 60°N to 20°N for January at 10 hPa have been computed. These computations have been done
219 for all three reanalyses (MERRA for period 1979-2012, ERA Interim for 1979-2012 and
220 NCEP/NCAR for 1958-2012). The results are shown in Fig. 1. The top panel shows results
221 for NCEP/NCAR, the middle panel for ERA Interim and the bottom panel for MERRA
222 reanalysis. The behaviour of different reanalyses is quite similar in major features despite the
223 different length of time intervals. Figure 1 reveals at 10 hPa for January a core of strong
224 poleward wind on the eastern hemisphere at the middle and higher latitudes. This poleward
225 wind changes into equatorward wind core on the western hemisphere at 10 hPa (at similar
226 amplitude as on the eastern hemisphere). Both the poleward and equatorward peaks (centres
227 of the cores in Fig. 1) are statistically significant at the 99% level for NCEP/NCAR
228 reanalysis. The results of similar analysis for 100 hPa are shown in Fig. 2. Generally, winds
229 are stronger at 10 hPa (up to 20 m/s) than at 100 hPa (up to 10 m/s). At 100 hPa there is a
230 five-core structure, which is much less pronounced than the two-core structure at 10 hPa. The
231 same analysis as in Fig. 1 is shown in Fig. 3 for July at 10 hPa. Figure 3 reveals no two-core
232 structure at 10 hPa for summer - it occurs only in winter. Winds in July are weaker than in

233 January and the distribution has no regular structure compared with January. We have done
234 the same analysis for the higher pressure level of 5 hPa (not shown) and the differences
235 between the eastern and western hemispheres (two-core structure) have been found to grow
236 with increasing height.

237 Figure 4 shows a climatology based on the NCEP/NCAR reanalysis over the period
238 1958-2012 for January at 10 hPa pressure level for data from 00 UTC (top panel), 06 UTC
239 (middle panel) and 12 UTC (bottom panel). There are almost no differences in the main
240 features. Therefore, we can conclude that the two-core structure with opposite meridional
241 winds is not caused by diurnal or semidiurnal tides. The other possibility for this structure
242 could be dynamical reasons, which are discussed in the next paragraph.

243 Wind field is closely associated with the distribution of geopotential height because of
244 dynamical reasons (principle of mass conservation, hydrostatic equation etc.). Figure 5 shows a
245 distribution of geopotential height at 10 hPa - again for all three reanalyses. The Aleutian
246 pressure high centred at about 40° - 55° N, 180° E is well developed at 10 hPa. This Aleutian
247 high can block the zonal winter eastward winds. This should result in poleward meridional
248 flow on the front (western) side and an equatorward meridional flow on the back (eastern)
249 side as a consequence of the flow along the strong anticyclone. Such a flow coincides with the
250 observed two-core structure at 10 hPa with the poleward meridional component of wind on
251 the eastern hemisphere and the equatorward meridional component on the western
252 hemisphere. The behaviour of zonal wind at 10 hPa, shown in Fig. 6 for all three reanalyses,
253 reveals substantial weakening of zonal wind in and around the region of the Aleutian pressure
254 height; together with strengthening of the meridional component, it results in non-zonal,
255 oblique wind flow. In some locations like 60° N, 135° E both wind components are
256 approximately equal. The summertime distribution of geopotential heights at 10 hPa does not
257 display any well-pronounced structure and, therefore, no pronounced structure is developed in

258 meridional wind (Fig. 3). The distribution of geopotential height resembles the five-core
259 structure in winds in Fig. 2 at 100 hPa on the western hemisphere but not on the eastern one.
260 But, again, this structure is much less pronounced than that at 10 hPa (not shown).

261 *3.2. Trends in meridional wind cores*

262 This analysis is focused on latitudes where the two-core structure at 10 hPa was
263 identified (50°N-60°N). It is based on the NCEP/NCAR reanalysis only. The trends in
264 meridional wind are shown in Table 1. We can identify change of trends in all four sectors
265 from a positive trend (core strengthening) for period 1970-1995 to a negative trend (core
266 weakening) for 1996-2012. The trends in core sectors (100°E-160°E and 140°W-80°W) are
267 significant at the 99% level for 1995-2012, and predominantly on the 95% level for 1970-
268 2012. Trends in the other two sectors are much smaller and statistically insignificant. The
269 turnaround of trends in total column ozone in the northern middle latitudes in the mid-1990s
270 (e.g. Harris et al., 2008) has an impact on the meridional wind cores – trends in cores also
271 alter, they change from positive before the ozone trend turnaround to negative after. We are
272 not going to speculate as to what extent this turnaround of meridional wind trends is caused
273 by dynamical factors, which is the main cause of the ozone trend turnaround. However,
274 impact of some external factors on trends in wind is investigated in the next section.

275

276

277 *3.3. Impact of solar cycle, SSW and QBO on trends in wind*

278 Further analysis (NCEP/NCAR reanalysis only, we can use longer period 1970-2012),
279 which has been done, is comparison between years in the solar cycle maximum and minimum
280 in different QBO phases and trends in different dynamical processes (SSW or no SSW years,

281 east or west QBO years). This analysis is also focused on latitudes where the two-core
282 structure at 10 hPa was identified (50°N-60°N). It should reveal potential connections
283 between solar cycle, stratospheric dynamics (wind speed) and wave activity driven SSW, all
284 under the potential influence of QBO. Stratospheric dynamics and chemistry is influenced by
285 changes in ozone concentration (see e.g. Table 1), so we analyse separately wind in the
286 periods 1970-1995, with decreasing ozone, and 1995-2012, with increasing ozone. Trends are
287 shown for different groups (with and without major SSW years and east or west QBO phase
288 years) for December-February (DJF), as the strongest two-core structure occurs in January.
289 We analyse the total horizontal wind as well as the meridional component separately to find
290 out which component is more affected by different drivers. The trends for meridional wind are
291 shown in Table 2. We can identify a turnaround of the trends in all four sectors for all four
292 groups (positive one for period 1970-1995, negative one for 1996-2012). There is little, if any,
293 systematic difference in trends between years with and without SSWs; perhaps the significant
294 trends are a little bit stronger in the years with SSWs. Similar conclusions can be drawn for
295 the impact of QBO; there is little dependence of trends on QBO, with perhaps slightly
296 stronger trends for the west phase of QBO.

297 The trends are significant at the 99% level (in a few cases only on the 95% level) in
298 the two sectors where the core structure occurs (100°E-160°E and 140°W-80°W). There are
299 only a few significant trends (95% level) in the other two sectors. There are generally stronger
300 negative significant trends (99 % level) in Table 1 than in Table 2 during the second period
301 (1996-2012) in the core-containing sectors.

302 The results on the connection of solar cycle and QBO with the total horizontal wind
303 speed are shown in the top panel of Table 3. At 10 hPa we can observe a positive difference
304 (of 2-5 m/s) between solar minimum and maximum for the west QBO in both sectors where
305 cores occur. The differences are significant at the 95% level. The differences are smaller and

306 insignificant in the other two wind sectors. The east QBO does not reveal a systematic or
307 significant difference. Moreover, sometimes wind in solar maximum is stronger than in solar
308 minimum. The differences between the QBO east and QBO west phase are negative in solar
309 minimum (up to 3 m/s) in all studied sectors. These differences are, again, mainly significant
310 in the two core sectors. Differences between the QBO east and QBO west phase in solar
311 maximum are mainly positive but insignificant.

312 The bottom panel shows the same analysis as the top one but for the v (meridional)
313 wind component. The differences are smaller than for the total horizontal wind. We cannot
314 find any specific features for all four groups. We can see only a few significant values in
315 different sectors.

316 The analysis was also done for each month separately and the largest differences have
317 been found in December and January. These results show that solar activity influences the
318 total horizontal wind (i.e. mainly zonal wind) mostly in higher parts of the stratosphere (10
319 hPa) and predominately in the two core sectors (not shown in the paper).

320

321

322 **4. Discussion**

323 The results on longitudinal distribution of the meridional and zonal components of
324 stratospheric wind show that the meridional wind forms a well pronounced two-core structure
325 at 10 hPa in winter. This two-core structure is revealed by NCEP/NCAR, ERA-Interim and
326 MERRA reanalyses in a very similar form, despite the different time periods used (Fig. 1).
327 The wintertime longitudinal distribution at 10 hPa can be explained neither by diurnal, nor by
328 semidiurnal tides, because there are no differences between the longitudinal distribution of

329 meridional winds at 00, 06 and 12 UTC (Fig. 4). However, the geopotential height analysis
330 reveals the reason for this longitudinal distribution. The well-developed large Aleutian high at
331 10 hPa (Fig. 5) can block the zonal flow (see Fig. 6) and pushes the winter eastward winds to
332 the pole (poleward) on the western side of the Aleutian pressure high and back, equatorward,
333 on its eastern side. A comparison of Figs. 1 and 6 shows that the zonal component of
334 stratospheric wind is almost equal to the meridional component in some areas in the cores.
335 This phenomenon could result in wave propagation changes in this part of the stratosphere (at
336 10 hPa, i.e. Matsuno, 1970, Kodera et al., 1990) and could affect other wave driven
337 phenomena like SSW. The results show that the deep (upper) branch of the Brewer-Dobson
338 circulation is affected by the longitudinal distribution of meridional wind, which can affect
339 the distribution of total ozone and of age of air in the middle stratosphere.

340 Therefore, Fig. 7 shows longitudinal distribution of ozone, and also temperature, at 10
341 hPa in the middle latitudes (20°-60°N). This distribution is consistent with the two-core
342 structure of meridional wind – in the eastern hemisphere, where the intensified poleward
343 meridional wind transports warmer air and more ozone towards higher latitudes (60°N), the
344 temperature and to a less extent ozone concentration are increasing; in the western hemisphere
345 core the opposite meridional transport reduces temperature and ozone at higher middle
346 latitudes. Thus all studied parameters, meridional wind, geopotential height, zonal wind,
347 temperature and ozone, agree in the main features of the longitudinal variation and provide an
348 internally consistent pattern of the longitudinal variation in the winter middle stratosphere (at
349 10 hPa) characterized by the two cores of strong meridional wind. This result illustrates
350 limitations of the applicability of the zonal mean approach.

351 In future studies, processes of the lower and higher levels of the atmosphere (below 100 hPa
352 and above 5 hPa) have to be analysed to find the main driver of these changes of meridional wind
353 direction. To our best knowledge the longitudinal structure of middle stratosphere circulation

354 at middle latitudes has not yet been studied except for Bari et al. (2013), who simulated with
355 the HAMMONIA model for 2001-2006, January a longitudinal structure of residual winds,
356 which resembles our results. They found impact from that longitudinal structure on the
357 Brewer-Dobson circulation and distribution of stratospheric ozone and water vapour (changes
358 in maximum and minimum of O₃ and H₂O and their distributions, their Figs. 7 and 8).
359 Investigation of the longitudinal dependence of stratospheric zonal winds during SSW events
360 with the model HAMMONIA (Miller et al., 2013, their Fig. 6) demonstrates the very
361 longitudinally asymmetric mean state of winter stratospheric zonal winds in HAMMONIA.
362 Moreover, the winds do not only evolve differently during the SSWs, the wind speeds were
363 found to differ by more than 20 m/s between the four locations at stratospheric altitudes
364 between 100 and 1 hPa.

365 We identify statistically significant trends in meridional wind (mostly at the 99 %
366 level) in both core sectors at 10 hPa (Table 1). These trends are positive (strengthening of
367 meridional wind) in 1970-1995 (decreasing ozone content) and negative (weakening of
368 meridional wind) in 1996-2012 (increasing ozone content) for both cores. The strengthening
369 of meridional wind in 1970-1995 (Table 1) and opposite trends/tendencies in 1996-2012 is
370 consistent with some strengthening/weakening of the blocking Aleutian pressure high. This is
371 confirmed by trends in the central part of the blocking Aleutian pressure high; +34.6 m/year
372 for 1970-1995 and -38.3 m/year for 1996-2012, both being significant at the 95% level. The
373 trends are mostly insignificant in the other two sectors (sector not affected by the two-core
374 structure, 160°E-140°W, 80°W-100°E). Reversal of trends in the mid-1990s occurred in both
375 meridional wind and ozone. However, ozone serves here as an indicator rather than as a
376 cause of the trend change. Statistical and modelling studies carried out in the European FP5
377 project CANDIDOZ show that the main cause of this change in ozone trends results from
378 changed dynamical behaviour like, e.g., EP flux, tropopause height and NAO index trends

379 (Harris et al., 2008). This conclusion is supported by behaviour of the ozone laminae
380 (Lastovicka et al., 2014).

381 The above results are the reason why, in section 3.3, we investigate the potential effect
382 of some dynamical factors (SSW and QBO), which could be behind the change of trends of
383 both ozone and wind. The change of the meridional wind trend (from positive to negative in
384 the mid-1990s) occurs independently of SSW or QBO (Table 2). We can connect this with
385 changes of ozone trends. The trends in core structure areas are significant (mainly at 99%
386 level) for all four SSW/QBO combinations (Table 2) as well as for all years trend (trend
387 including all seasons, Table 1). In areas not containing the core structure, more significant
388 trends (95% level) occur for years with SSWs than without major SSWs. This result could
389 indicate that the unusual conditions in the stratosphere during an SSW can affect meridional
390 wind trends (B-D circulation and ozone transport) even in areas where meridional wind is
391 weak.

392 According to Shindell et al. (1999) the changes of the upper stratospheric wind are
393 caused partly by changes in the solar irradiance. The impact of the 11-yr solar cycle,
394 sometimes in the combination with the QBO, on the stratosphere has been described in many
395 papers (i.e. Salby and Callahan, 2000, Labitzke and Kunze, 2009, Limpasuvan et al. 2004,
396 Naito and Hirota, 1997, Labitzke and van Loon, 1988). The influence of solar activity on the
397 total horizontal wind as well as the meridional component is shown in Table 3. Our results
398 agree with the results of other authors (mentioned above) but we specify dependence of solar
399 effect on longitude. The most statistically significant differences in the total horizontal wind
400 can be found again in the two core sectors. The differences are larger at higher latitudes. This
401 result agrees with previous studies (Labitzke and Kunze, 2009, Labitzke and van Loon, 1988)
402 that higher latitudes are more affected by changes in solar activity. The analysis of the

403 meridional component does not show any specific features so we can conclude that solar
404 activity affects mainly the total horizontal wind and its zonal component.

405

406 **5. Conclusions**

407 Based on data from reanalyses NCEP/NCAR, ERA-Interim and MERRA, the
408 longitudinal distribution of meridional component of stratospheric wind in winter (January)
409 has been examined for 20-60°N. It reveals a well pronounced longitudinal distribution of
410 meridional wind at latitudes above 45°N with two cores of strong but opposite meridional
411 winds, one in each hemisphere (eastern and western) at 10 hPa, and a much less pronounced
412 five-core structure at 100 hPa. All three reanalyses provide the same pattern. In summer, such
413 a well-pronounced core structure is absent. The two-core structure at 10 hPa is not caused by
414 tides, as no differences exist between 00, 06 and 12 UTC results. We have identified the
415 strong and well-developed large Aleutian pressure high at 10 hPa, which is capable of
416 explaining qualitatively the two-core structure in the longitudinal distribution of meridional
417 wind. The longitudinal distribution of zonal wind, temperature and total ozone column is
418 consistent with that of meridional wind and geopotential height, i.e. the middle stratosphere as
419 a whole displays a significant longitudinal distribution at higher middle latitudes. Our results
420 illustrate limitations of the approach via zonal mean values when studying the northern
421 midlatitude middle stratosphere (i.e. the zonal mean of meridional component in middle
422 latitudes masks the two-core structure and probably the significant trend).

423 The trends of meridional wind are found to be significant in the two core sectors
424 independently of SSW or QBO. They are predominantly much weaker and insignificant in
425 sectors not containing the two cores. In the period of ozone depletion deepening (1970-1995),
426 the meridional wind in the cores intensifies, whereas in the period of recovering ozone

427 concentration (1996-2012) it weakens. There is no pronounced dependence of these trends on
428 the occurrence of sudden stratospheric warming and on the phase of QBO. However, there is
429 an indirect dependence of wind on QBO, as the influence of solar cycle can be seen mainly
430 for the west phase of QBO.

431 Future investigations should be focused on altitudinal and seasonal extent of the two-
432 core structure in meridional wind and related long-term trends.

433

434

435 **Acknowledgments**

436 Authors acknowledge support by the Grant Agency of the Czech Republic, grants
437 P209/10/1792 and 15-03909S, by the Ministry of Education, Youth and Sports of the Czech
438 Republic, grant LD 12070, and by the COST ES1005 project (TOSCA).

439

440

441

442

443 **References**

444 Baldwin, M.P., and Dunkerton, T.J.: Propagation of the arctic oscillation from the
445 stratosphere to the troposphere, *J. Geophys. Res.*, 104, 30937-30946, 1999.

446 Baldwin, M., Shuckburgh, D. Norton, E., Thompson, and W., Gillett, G.: Weather from the
447 Stratosphere? *Science*, 301, 317-318, 2003.

448 Baron, P., Murtagh, D. P., Urban, J., Sagawa, H., Ochiai, S., Kasai, Y., Kikuchi, K.,
449 Khosrawi, F., Kornich, H., Mizobuchi, S., Sagi, K and Yasui, M.: Observation of
450 horizontal winds in the middle-atmosphere between 30° S and 55° N during the northern
451 winter 2009–2010, *Atmos. Chem. Phys.*, 13, 6049-6064, doi:10.5194/acp-13-6049-2013,
452 2013.

453 Bari, D., Gabriel, A., Körnich, H., Peters, D. W. H.: The effect of zonal asymmetries in the
454 Brewer-Dobson circulation on ozone and water vapor distributions in the northern middle
455 atmosphere, *J. Geophys. Res. Atmos.*, 118, 3447-3466, doi: 10.1029/2012JD017709, 2013

456 Butchart, N.: The Brewer-Dobson circulation, *Rev. Geophys.*, 52, 157-184, doi:
457 10.1002/2013RG000448, 2014.

458 Charlton, A. J., and Polvani, L. M.: A new look at stratosphere sudden warmings. Part I.
459 *Climatology and Modeling Benchmarks*, *J. Atmos. Sci.*, 20, 449-469, 2007

460 Deckert, R., and Dameris, M.: Higher tropical SSTs strengthen the tropical upwelling via
461 deep convection, *Geophys. Res. Lett.*, 35, L10813, doi: 10.1029/2008GL033719, 2008.

462 Dee, D. P., Uppala, S. M., Simmons, A. J., Berrisford, P., Poli, P., Kobayashi, S., Andrae, U.,
463 Balmaseda, M. A., Balsamo, G., Bauer, P., Bechtold, P., Beljaars, A. C. M., van de Berg,
464 L., Bidlot, J., Bormann, N., Delsol, C., Dragani, R., Fuentes, M., Geer, A. J., Haimberger,
465 L., Healy, S. B., Hersbach, H., Hólm, E. V., Isaksen, L., Kållberg, P., Köhler, M.,
466 Matricardi, M., McNally, A. P., Monge-Sanz, B. M., Morcrette, J.-J., Park, B.-K., Peubey,
467 C., de Rosnay, P., Tavolato, C., Thépaut, J.-N., and Vitart, F.: The ERA-Interim reanalysis:
468 configuration and performance of the data assimilation system, *Q. J. Roy. Meteorol. Soc.*,
469 137, 553–597, 2011.

470 Engel, A., Möbius, T., Bönisch, H., Schmidt, U., Heinz, R., Levin, I., Atlas, E., Aoki, S.,
471 Nakazawa, T., Sugawara, S., Moore, F., Hurst D., Elkins J., Schauffler S., Andrews A.,

472 and Boering K.: Age of stratospheric air unchanged within uncertainties over the past 30
473 yr. *Nat. Geosci.*, 2, 28–31, doi:10.1038/ngeo388, 2009.

474 Gray, L.J., Beer, J., Geller, M., Haigh, J.D., Lockwood, M., Matthes, K., Cubasch, U.,
475 Fleitmann, D., Harrison, G., Hood, L., Luterbacher, J., Meehl, G.A., Shindell, D., van
476 Geel, B., and White, W.: Solar influences on climate, *Rev. Geophys.*, 48, RG4001, doi:
477 10.1029/2009RG000282, 2010.

478 Hamilton, K., Vial, F., and Stenchikov, G.: Longitudinal variation of the stratospheric quasi-
479 biennial oscillation, *J. Atmos. Sci.*, 61 (4), 383-402, 2004.

480 Harris, N. R. P., Kyrö, E. Staehelin, J., et al.: Ozone trends at northern mid- and high
481 latitudes — A European perspective, *Ann. Geophys.*, 26, 1207–1220, doi: 10.5194/angeo-
482 26-1207-2008, 2008.

483 Hartmann, D. L., Wallace, J. M., Limpasuvan, V., Thompson, D. W., and Holton, J. R.: Can
484 ozone depletion and global warming interact to produce rapid climate change? *Proc. Nat.*
485 *Acad. Sci.*, 97(4), 1412-1417, 2000.

486 Hildebrand, J., Baumgarten, G., Fiedler, J., Hoppe, U.-P., Kaifler, B., Lubken, F.-J., and
487 Williams, B. P.: Combined wind measurements by two different lidar instruments in the
488 Arctic middle atmosphere, *Atmos. Meas. Tech.*, 5, 2433–2445, 2012.

489 Holton, J. R., and Alexander, M. J. The role of waves in transport circulation of the middle
490 atmosphere. *Geophys. Monogr. Ser.*, vol. 123, AGU, Washington DC, 21-35, 2000.

491 Kistler, R., Collins W. Kalnay, E., et al. The NCEP 50-year reanalysis: Monthly means
492 CDrom and documentation. *Bull. Am. Meteorol. Soc.* 82 (2), 247-267, 2001.

493 Kodera, K., Yamazaki, K., Chiba, M., & Shibata, K.: Downward propagation of upper
494 stratospheric mean zonal wind perturbation to the troposphere. *Geophys. Res. Lett.*, 17(9),
495 1263-1266, doi: 10.1029/GL017i009p01263, 1990.

496 Kozubek, M., Laštovička, J., and Križan, P.: Differences in mid-latitude stratospheric winds

497 between reanalysis data and versus radiosonde observations at Prague, *Ann. Geophys.*, 32,
498 353-366, doi: 10.5194/angeo-32-353-2014, 2014.

499 Labitzke, K., and van Loon, H.: Associations between the 11-year solar cycle, the QBO and
500 the atmosphere: Part I. The troposphere and stratosphere in the Northern Hemisphere
501 winter, *J. Atmos. Terr. Phys.*, 50, 197–206, 1988

502 Labitzke, K., and Kunze, M.: Variability in the stratosphere: The Sun and the QBO,
503 in *Climate and Weather of the Sun-Earth System (CAWSES): Selected Papers from the*
504 *Kyoto Symposium* edited by K. S. T. Tsuda, R. Fujii, and M. Geller, pp. 257–278,
505 TERRAPUB, Tokyo, 2009.

506 Lastovicka, J., Solomon, S.C., and Qian, L.: Trends in the Neutral and Ionized Upper
507 Atmosphere, *Space Sci. Rev.*, 168, 113–145, doi: 10.1007/s11214-011-9799-3, 2012.

508 Lastovicka, J., Krizan, P., and Kozubek, M.: Long-term trends in the northern extratropical
509 ozone laminae with focus on European stations, *J. Atmos. Sol.-Terr. Phys.*, 120, 88-95,
510 <http://dx.doi.org/10.1016/j.jastp.2014.09.006>, 2014.

511 Limpasuvan, V., Thompson, D. W., and Hartmann, D. L. The life cycle of the Northern
512 Hemisphere sudden stratospheric warmings. *J. Clim.*, 17(13), 2584-2596, 2004.

513 Lin, P., and Fu, Q.: Changes in various branches of the Brewer–Dobson circulation from an
514 ensemble of chemistry climate models. *J. Geophys. Res. Atmos.*, 118(1), 73-84, doi:
515 10.1029/2012JD018813, 2013.

516 Marshall, A. G., and Scaife, A. A. Impact of the QBO on surface winter climate. *J. Geophys.*
517 *Res. Atmos.*, 114, D18, doi: 10.1029/2009JD011737, 2009

518 Manney, G. L., Santee, M. L., Rex, M., Livesey, N. J., Pitts, M. C., Veefkind, P., Nash, E.
519 R., Wohltmann, I., Lehmann, R., Froidevaux, L., Poole, L. R., Schoeberl, M. R., Haffner,
520 D. P., Davies, J., Dorokhov, V., Gernandt, H., Johnson, B., Kivi, R., Kyrö, E., Larsen,
521 N., Levelt, P. F., Makshtas, A., McElroy, C. T., Nakajima, H., Parrondo, M. C., Tarasick,

522 D. W., von der Gathen, P., Walker, K. A., and Zinoviev, N. S.: Unprecedented Artic loss
523 in 2011, *Nature*, 478, 469-475, doi: 10.1038/nature10556, 2011

524 Matsuno, T.: Vertical propagation of stationary planetary waves in the winter Northern
525 Hemisphere. *J. Atmos. Sci.*, 27(6), 871-883, 1970.

526 Miller, A., Schmidt, H., and Bunzel, F.: Vertical coupling of the middle atmosphere during
527 stratospheric warming events. *J. Atmos. Sol.-Terr. Phys.*, 97, 11-21,
528 <http://dx.doi.org/10.1016/j.jastp.2013.02.008>, 2013.

529 Mlch, P.: Total ozone response to major geomagnetic storms during non-winter periods.
530 *Studia geoph. Geod.*, 38 (4), 423-429, 1994.

531 Monier, E. and Weare, B. C.: Climatology and trends in the forcing of the stratospheric ozone
532 transport., *Atmos. Chem. Phys.*, 11, 6311-6323, doi: 10.5194/acp-11-6311-2011, 2011a.

533 Monier, E. and Weare, B. C.: Climatology and trends in the forcing of the stratospheric zonal-
534 mean flow. *Atmos. Chem. Phys.*, 11, 12751-12771, doi: 10.5194/acp-11-12751-2011,
535 2011b.

536 Naito, Y., and Hirota, I. Interannual variability of the northern winter stratospheric circulation
537 related to the QBO and the solar cycle. *Journal of the Meteorological Society of*
538 *Japan*, 75(4), 925-937, 1997

539 Oberländer, S., Langematz, U., and Meul, S.: Unravelling impact factors for future changes in
540 the Brewer-Dobson circulation. *J. Geophys. Res. Atmos.*, 118, 10,296-10,312, doi:
541 10.1002/jgrd.50775, 2013.

542 Oman, L., Waugh, D. W., Pawson, S., Stolarski, R. S., and Newman, P. A.: On the influence
543 of anthropogenic forcings on changes in the stratospheric mean age. *J. Geophys. Res.*
544 *Atmos.*, 114, D03105, doi: 10.1029/2008JD010378, 2009.

545 Ortland, D. A., Skinner, W. R., Hays, P. B., Burrage, M. D., Lieberman, R. S., Marshall, A.
546 R., and Gell, D. A.: Measurements of stratospheric winds by the High Resolution Doppler
547 Imager. *J. Geophys. Res.*, 101, 10351–10363, 1996.

548 Pommereau, J.-P., Goutail, F., Lefèvre, F., Pazmino, A., Adams, C., Dorokhov, V., Eriksen,
549 P., Kivi, R., Stebel, K., Zhao, X., and van Roozendaal, M.: Why unprecedented ozone loss
550 in the Arctic in 2011? Is it related to climate change? *Atmos. Chem. Phys.*, 13, 5299- 5308,
551 doi: 10.5194/acp-13-5299-2013, 2013.

552 Ray, E. A., Moore, F. L., Rosenlof, K. H., Davis, S. M., Sweeney, C., Tans, P., Wang, T.,
553 Elkins, J. W., Bönisch, H., Engel, A., Sugawara, S., Nakazawa, T., Aoki, S.: Improving
554 stratospheric transport trend analysis based on SF₆ and CO₂ measurements, *J. Geophys.*
555 *Res. Atmos.*, 119 (24), doi: 10.1002/2014JD021802, 2014.

556 Rüfenacht, R., Kampf, N., and Murk, A.: First middle atmospheric zonal wind profile
557 measurements with a new ground-based microwave Doppler-spectro-radiometer, *Atmos.*
558 *Meas. Tech.*, 5, 2647–2659, 2012

559 Salby, M., Callahan, P.: Connection between the Solar Cycle and the QBO: The missing link,
560 *J. Clim.*, 13(14), 2652-2662, 2000.

561 Scaife, A. A., Spanghel, T., Fereday, D. R., Cubasch, U., Langematz, U., Akiyoshi, H.,
562 Slimane, B., Breasicke, P., Butchard, N., Chipperfield, M. P., Gettelman, A., Hardiman, S.
563 C., Michou, M., Rozanov, E. and Shepherd, T. G.: Climate change projections and
564 stratosphere–troposphere interaction. *Clim. Dynamics*, 38(9-10), 2089-2097, 2012.

565 Shepherd, T.G. Transport in the middle atmosphere. *J. Meteorol. Soc. Jpn. II*, 85B,
566 165-191, 2007.

567 Shepherd, T.G. Dynamics, stratospheric ozone, and climate change. *Atmos. Ocean*, 46,
568 117-138, 2008.

569 Shindell, D., Rind, D., Balachandran, N., Lean, J., and Lonergan, P.: Solar cycle variability,
570 ozone, and climate. *Science*, 284(5412), 305-308, 1999.

571 Sigmond, M., Scinocca, J. F., and Kushner, P. J. Impact of the stratosphere on the tropospheric
572 climate change. *Science*, 301, 317-318, 2008.

573 Stiller, G. P., von Clarmann, T., Haene, F., Funke, B., Glatthor, N., Grabowski, U., Kellmann,
574 S., Kiefer, M., Linden, A., Lossow, S., and Lopez-Puertas, M.: Observed temporal
575 evolution of global mean age of stratospheric air for the 2002 to 2010 period. *Atmos.*
576 *Chem. Phys.*, 12, 3311–3331, doi: 10.5194/acp-12-3311-2012, 2012.

577 Wang, L., and Chen, W. Downward arctic oscillation signal associated with moderate weak
578 stratospheric polar vortex and the cold December 2009. *Geophys. Res. Lett.*, 37, L09707,
579 doi: 10.1029/2010GL042659, 2010.

580 Waugh, D. W., and Hall, T. M.: Age of stratospheric air: Theory, observations and models.
581 *Rev. Geophys.*, 40, no. 4, 1010, doi: 10.1029/200RG000101, 2002

582 Weare, B. C.: Tropospheric-stratospheric wave propagation during El Niño-Southern
583 Oscillation. *J. Geophys. Res.*, 115, D18122, doi: 10.1029/2009JD013647, 2010.

584

585

586

587

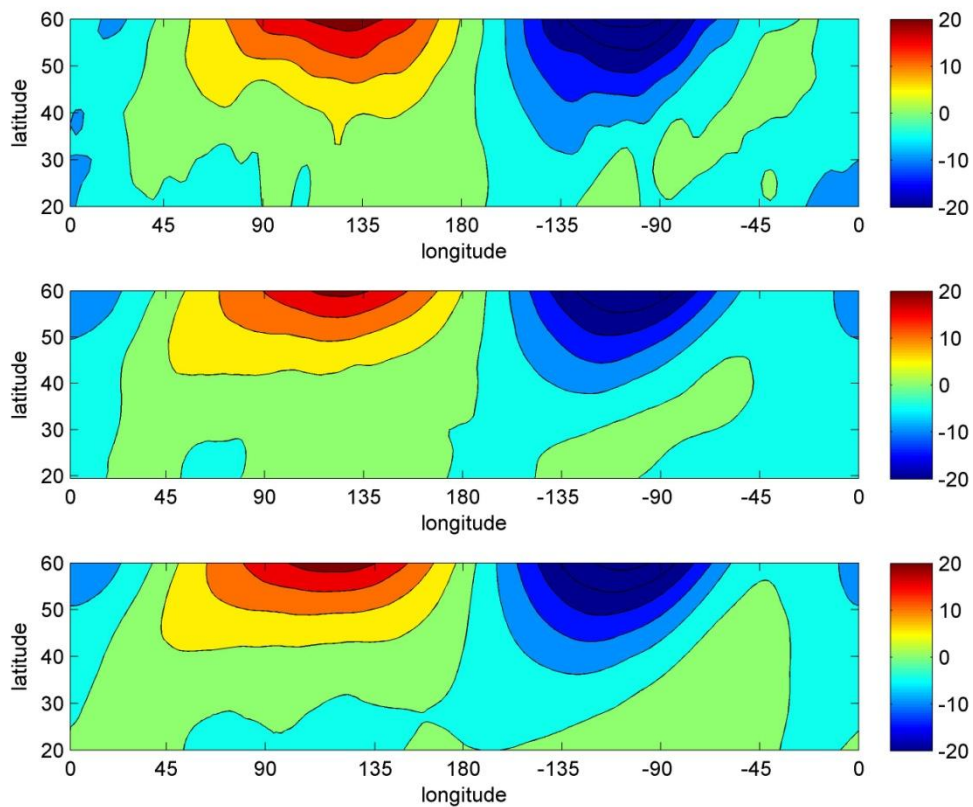
588

589

590

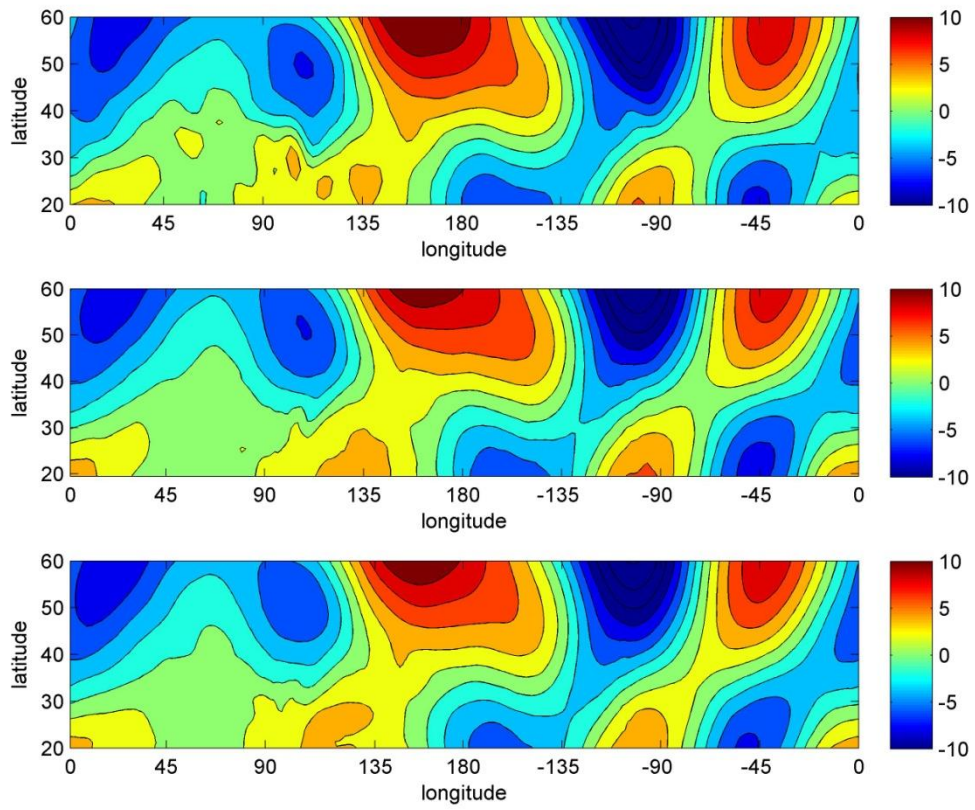
591

592 **Figure captions:**



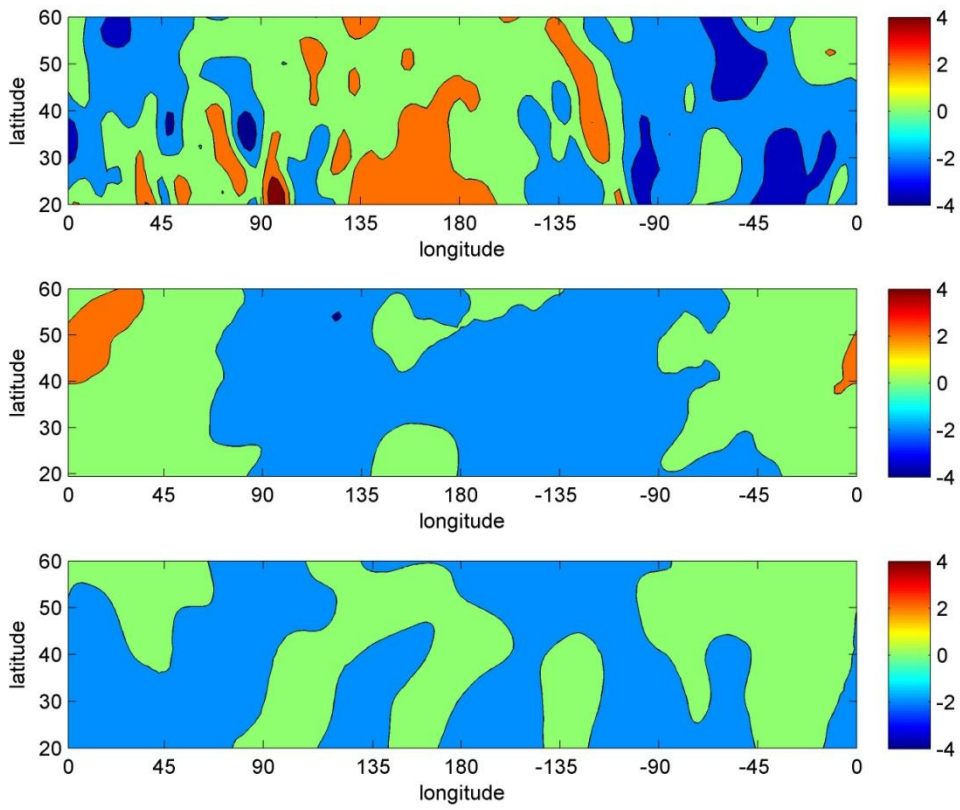
593

594 **Figure 1.** Plot of average meridional wind speed (m/s) component for January, 20-60°N,
595 180°E-180°W, 10 hPa. Top panel NCEP/NCAR (1958-2012), middle ERA Interim (1979-
596 2012), and bottom MERRA (1979-2012). Positive values (poleward wind - red), negative
597 values (equatorward wind – blue).



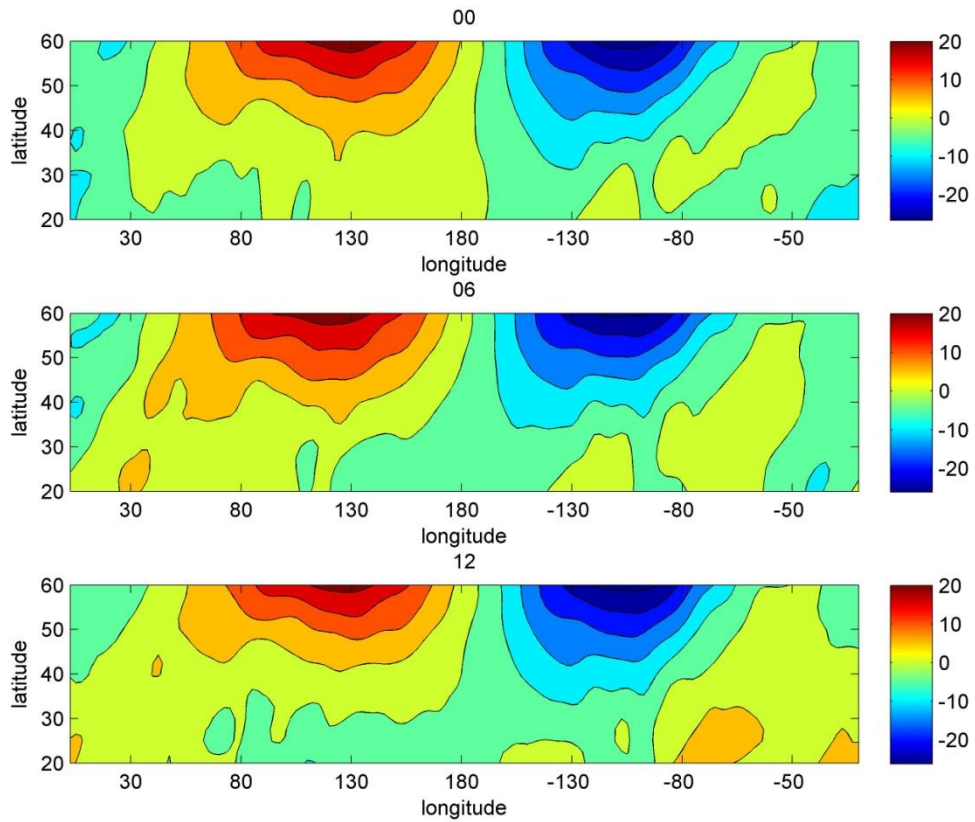
598

599 **Figure 2.** The same as Fig.1 but for 100 hPa.



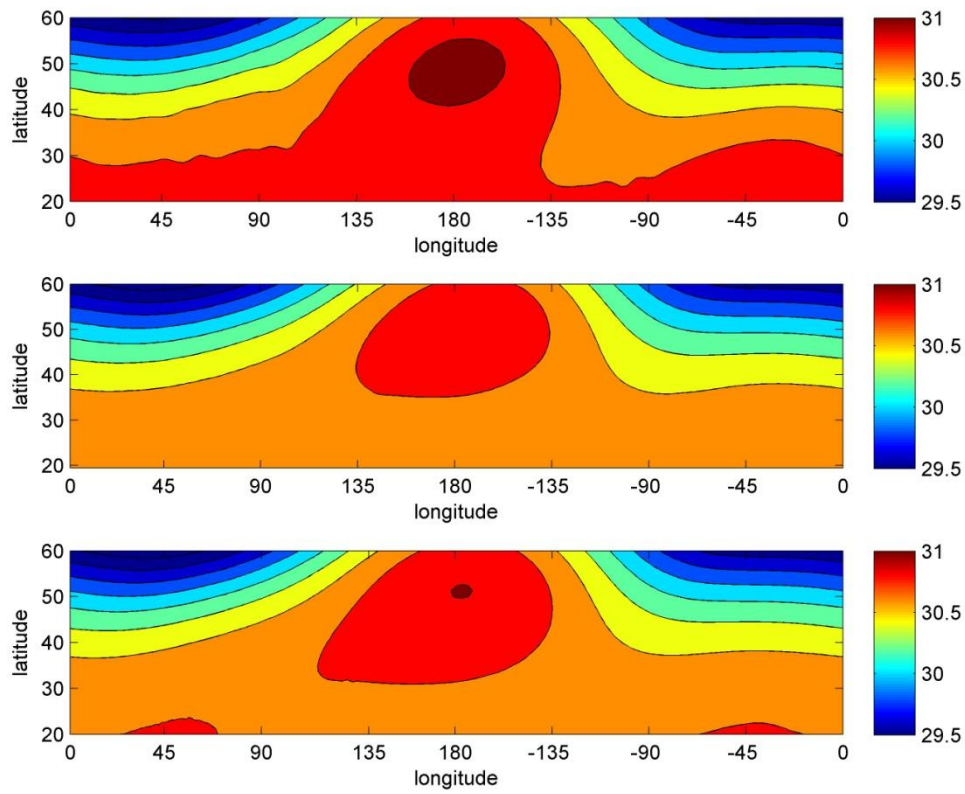
600

601 **Figure 3.** The same as Fig. 1 but for July. Positive values (poleward wind - red), negative
 602 values (equatorward wind - blue).



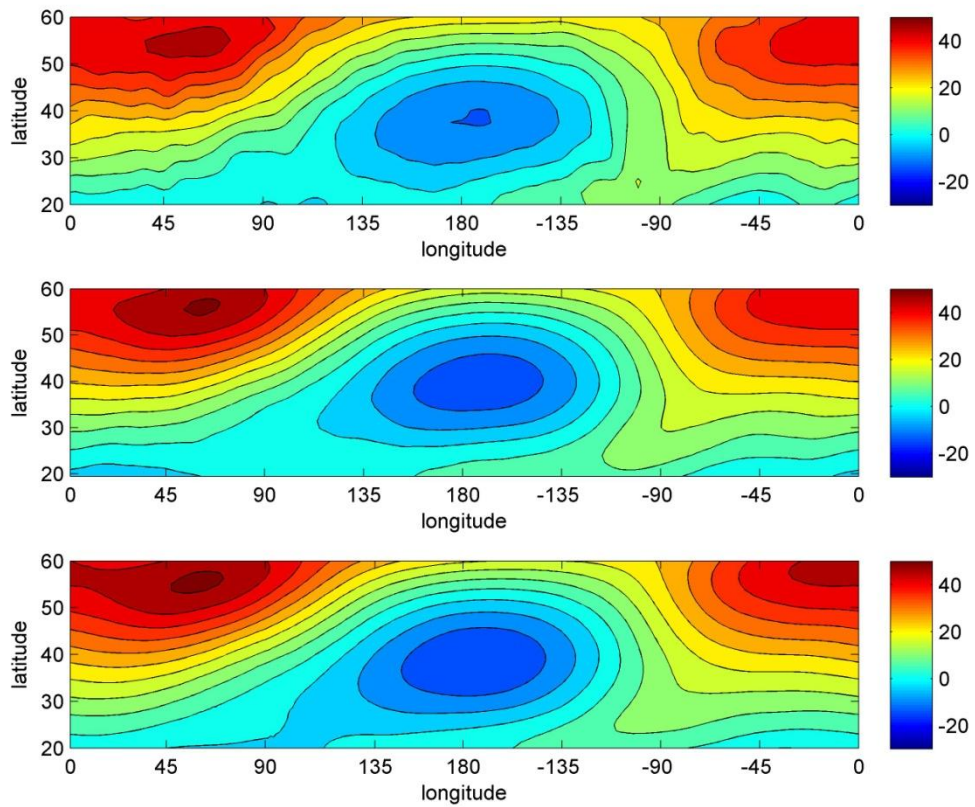
603

604 **Figure 4.** Plot of average meridional wind speed (m/s) component at 10 hPa for January,
 605 1958-2012, 20-60°N, 180°E-180°W. Top panel 00 UTC, middle 06 UTC, and bottom 12
 606 UTC. Positive values (poleward wind - red), negative values (equatorward wind - blue),
 607 NCEP/NCAR reanalysis only.



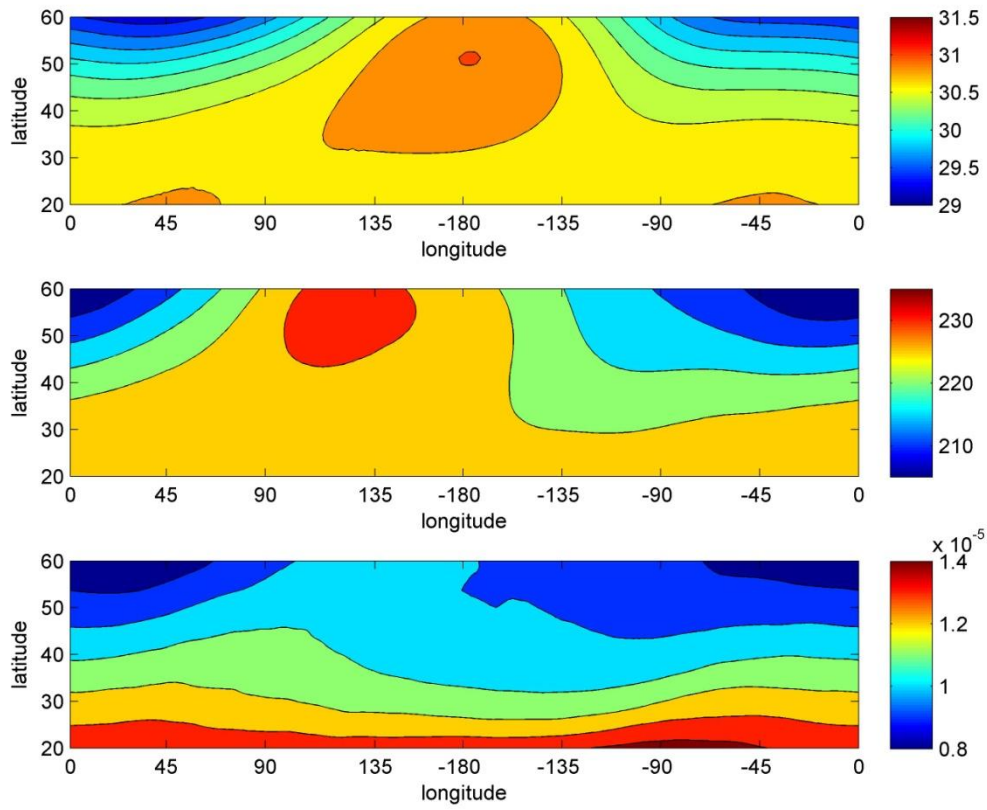
608

609 **Figure 5.** Plot of average geopotential height (km) for January, 1958-2012, 20-60°N, 180°E-
 610 180°W. Top panel NCEP/NCAR (1958-2012), middle ERA Interim (1979-2012), and bottom
 611 MERRA (1979-2012).



612

613 **Figure 6.** Plot of average zonal wind speed (m/s) component for January, 20-60°N, 180°E-
 614 180°W, 10 hPa. Top panel NCEP/NCAR (1958-2012), middle ERA Interim (1979-2012), and
 615 bottom MERRA (1979-2012). Positive values (eastward wind - red), negative values
 616 (westward wind - blue).



617

618 **Figure 7.** Plot of average geopotential height (km, top panel), temperature (K, middle panel)

619 and ozone mixing ratio (ppmv, bottom panel) for January, 20-60°N, 180°E-180°W, 10 hPa.

620

621

622

623

624

625

626

627

628 **Table 1.** Winter (December-February) trends (m/s per year) of meridional wind speed for two
629 periods (1970-1995 and 1996-2012). Pressure level 10 hPa. 70-95 means 1970-1995 and 95-
630 12 means 1995-2012 Trends significant at the 99% level are highlighted by bold; trends
631 significant at the 95% level are in italics. Sectors 100°-160°E and 140°-80°W are the sectors
632 with cores in meridional wind.
633

| | | 10 hPa | | | | | | | | | | | |
|----------|--------------|-------------------------|-------------------------|------------------------|------------------------|-----------------|-------------------------|------------------------|------------------------|-------------------------|-------------------------|------------------------|------------------------|
| latitude | sector | 50°N | | | | 55N | | | | 60°N | | | |
| | | 100° E- 160° E | 160° E- 140° W | 140° W- 80° W | 80°W - 100° E | 100°E- 160°E | 160° E- 140° W | 140° W- 80° W | 80° W- 100° E | 100° E- 160° E | 160° E- 140° W | 140° W- 80° W | 80° W- 100° E |
| | 70-95 | 0.42 | 0.10 | <i>0.39</i> | 0.07 | 0.48 | 0.11 | <i>0.42</i> | 0.03 | <i>0.47</i> | 0.09 | <i>0.42</i> | 0.04 |
| | 95-12 | -0.71 | -0.15 | -0.68 | -0.09 | -0.68 | -0.19 | -0.74 | -0.06 | -0.74 | -0.12 | -0.67 | -0.10 |

634
635
636
637
638
639
640
641
642
643

644 **Table 2.** Winter (December-February) trends (m/s per year) of the meridional wind speed for
645 two periods (1970-1995 and 1996-2012). Major SSW- only years when the major SSWs
646 (according to WMO definition) occur; no SSW – years when no major SSW occurs; east
647 QBO - only years under the east phase of QBO ; west QBO - only years under the west phase
648 of QBO. Pressure level 10 hPa. 70-95 means 1970-1995 and 95-12 means 1995-2012. Trends
649 significant at the 99% level are highlighted by bold numbers; trends significant at the 95%
650 level are in italics.

| | | 10 hPa | | | | | | | | | | | | | |
|----------|-----------------|----------------|--------------|--------------|--------------|----------------|--------------|--------------|--------------|-------------|----------------|--------------|-------|-----|-----|
| Latitude | | 50°N | | | | 55N | | | | 60°N | | | | | |
| sector | 100°E- 160°E | 160°E | 140°W- | 80°W- | 100°E | 160°E | 140°W - | 80°W- | 100°E- | 160°E- | 140°W- | 80°W- | major | SSW | |
| | | - 140° W | 80°W | 100°E | - 160°E | - 140° W | 80°W | 100°E | 160°E | 140°W | 80°W- 100°E | no | | | SSW |
| 70-95 | 0.52 | <i>0.21</i> | <i>0.49</i> | 0.15 | 0.57 | 0.15 | 0.54 | 0.12 | 0.6 | 0.11 | 0.55 | 0.1 | | | |
| 95-12 | -0.61 | -0.19 | -0.63 | -0.1 | -0.61 | <i>-0.27</i> | -0.67 | <i>-0.24</i> | -0.64 | -0.22 | -0.59 | <i>-0.26</i> | | | |
| 70-95 | 0.39 | <i>0.23</i> | 0.46 | <i>0.2</i> | 0.43 | 0.19 | 0.51 | 0.15 | 0.49 | 0.16 | 0.56 | <i>0.18</i> | | | |
| 95-12 | -0.71 | -0.08 | -0.42 | -0.05 | -0.6 | -0.11 | -0.49 | -0.08 | -0.64 | -0.13 | -0.56 | -0.1 | | | |
| 70-95 | 0.37 | 0.14 | 0.35 | 0.09 | <i>0.39</i> | <i>0.17</i> | 0.42 | <i>0.19</i> | 0.43 | 0.19 | 0.48 | 0.23 | | | |
| 95-12 | -0.44 | <i>-0.24</i> | -0.4 | <i>-0.19</i> | -0.48 | -0.16 | -0.46 | -0.11 | -0.53 | -0.12 | -0.51 | -0.09 | | | |
| 70-95 | 0.34 | <i>0.19</i> | 0.49 | <i>0.2</i> | 0.41 | <i>0.24</i> | 0.55 | 0.21 | <i>0.39</i> | <i>0.25</i> | 0.59 | <i>0.27</i> | | | |
| 95-12 | -0.5 | -0.08 | -0.64 | -0.04 | -0.54 | -0.12 | -0.62 | -0.09 | -0.57 | -0.17 | -0.68 | -0.12 | | | |

651

652

653

654

655

656

657 **Table 3.** Winter (December-February) differences of wind speed (m/s) for different latitudes
658 and sectors during the whole period. Top panel shows the total horizontal wind speed for 10
659 hPa, bottom panel the v (meridional) wind component for 10 hPa. Min-east: years under solar
660 minimum and the east phase of QBO conditions; min-west: years under solar minimum and
661 the west phase of QBO; the same for solar maximum conditions. Significant differences at the
662 95% level are highlighted by bold numbers.

| | 50°N | | | | 55°N | | | | 60°N | | | | latitude sector |
|---------------------------|---------------------------|-------------------------|----------------------------|--------------------|-------------------------|-------------------------|------------------------|--------------------|-------------------------|-------------------------|------------------------|--------------------|--------------------|
| | 100° E- 160° E | 160° E- 140° W | 140° W- 80°W 80°W | 80°W -100° E | 100° E- 160° E | 160° E- 140° W | 140° W- 80° W | 80°W -100° E | 100° E- 160° E | 160° E- 140° W | 140° W- 80° W | 80°W -100° E | |
| | (min/east)- (min/west) | -1.07 | -0.08 | -1.47 | -0.03 | -1.89 | -0.28 | -1.73 | -0.23 | -2.77 | -0.57 | -2.05 | |
| (max/east)- (max/west) | 0.33 | -0.27 | 1.26 | -0.46 | 0.66 | -0.42 | 1.17 | -0.44 | 1.04 | -0.18 | 0.76 | -0.27 | |
| (min/west)- (max/west) | 2.02 | 0.38 | 1.39 | 0.51 | 2.76 | 0.81 | 1.84 | 0.72 | 3.19 | 1.08 | 2.23 | 1.01 | |
| (min/east)- (max/east) | 0.62 | 0.96 | -1.36 | 1.02 | -0.39 | 0.75 | -1.19 | 0.81 | -0.71 | 0.64 | -0.92 | 0.56 | |
| (min/east)- (min/west) | -0.01 | 0.34 | -0.63 | 0.60 | -0.11 | -0.29 | -0.73 | 0.79 | -0.26 | 1.14 | -0.84 | 1.12 | 10 hPa v |
| (max/east)- (max/west) | -0.38 | 0.2 | 0.15 | 0.09 | -0.40 | -0.52 | 0.14 | 0.10 | -0.43 | 0.18 | 0.17 | 0.14 | |
| (min/west)- (max/west) | -0.17 | 0.42 | 1.17 | -0.73 | -0.20 | -0.17 | 1.39 | -0.86 | -0.18 | -0.95 | 1.57 | -0.99 | |
| (min/east)- (max/east) | 0.19 | -0.29 | 0.39 | -0.22 | 0.09 | -0.11 | 0.49 | -0.17 | -0.01 | -0.17 | 0.57 | -0.11 | |

663

664

665

666

667

668